

Original Article

Repurposing of posaconazole as a hedgehog/SMO signaling inhibitor for embryonal rhabdomyosarcoma therapy

Jingkai Sun^{1,2*}, Wenfeng Lin^{2*}, Chaoming Li^{1,2}, Hideo Ueki², Ruizhi Xue², Takuya Sadahira², Hao Hu³, Koichiro Wada², Na Li³, Chunxiao Liu¹, Motoo Araki², Abai Xu¹, Peng Huang^{1,2,4}

¹Department of Urology, Zhujiang Hospital, Southern Medical University, Guangzhou, China; ²Department of Urology, Okayama University Graduate School of Medicine, Dentistry and Pharmaceutical Sciences, Okayama, Japan; ³Laboratory of Medical Systems Biology, Guangzhou Women and Children's Medical Center, Guangzhou Medical University, Guangzhou, China; ⁴Okayama Medical Innovation Center, Okayama University, Okayama, Japan. *Equal contributors and co-first authors.

Received June 10, 2021; Accepted July 16, 2021; Epub September 15, 2021; Published September 30, 2021

Abstract: Posaconazole (POS) is a novel antifungal agent, which has been repurposed as an anti-tumor drug for its potential inhibition of Hedgehog signaling pathway. Hedgehog pathway is reported to be abnormally activated in embryonal rhabdomyosarcoma (ERMS), this study aimed to reveal whether POS could inhibit Hedgehog signaling pathway in ERMS. Following POS treatment, XTT viability assay was used to determine the cell proliferation of ERMS cell lines. Protein changes related to Hedgehog signaling, cell cycle and autophagy were detected by Western blot. The cell cycle distribution was analyzed by flow cytometry. Moreover, a subcutaneous tumor mouse model of ERMS was established to assess the anti-tumor effect of POS. POS was found to inhibit tumor progression by inducing G0/G1 arrest and autophagy of RD, RMS-YM, and KYM-1 cells dose-dependently. Western blot demonstrated that POS downregulated the expressions of SMO, Gli1, c-Myc, CDK4, and CDK6, while upregulated the expressions of autophagy-related proteins. Immunofluorescence microscopy revealed a significant increase of LC3B puncta in POS-treated ERMS cells. Furthermore, POS treatment led to a significant inhibition of tumor growth in mice bearing ERMS. Our findings could provide a theoretical basis and have important clinical implications in developing POS as a promising agent against ERMS by targeting Hedgehog pathway.

Keywords: Posaconazole, cell cycle, autophagy, rhabdomyosarcoma, hedgehog proteins

Introduction

Rhabdomyosarcoma (RMS) is the most common soft tissue sarcoma in children and is regarded as one of the main pediatric solid tumors. RMS can be classified into two main subtypes, embryonal RMS (ERMS) and alveolar RMS (ARMS). The current standard treatment of ERMS is mainly multidisciplinary with a combination of surgical tumor excision, systemic chemotherapy comprised of vincristine, actinomycin D, and cyclophosphamide or ifosfamide and radiation therapy. Although some localized ERMS lesions can be cured, the prognosis of metastatic or recurrent ERMS is not ideal [1, 2]. Especially for the treatment of urinary ERMS such as bladder and prostate ERMS, it remains a challenge to significantly improve survival through the main mode of extensive

surgical resection after chemotherapy [3]. And the multidisciplinary treatment may impair the bladder function and erectile function [3]. Therefore, it is still necessary to explore new ERMS therapies with meliorative oncological and functional outcomes.

Hedgehog signaling plays an essential role in regulating a series of embryonic development processes, such as cell growth, differentiation and organogenesis [4-6]. Related studies have demonstrated that the aberrant activation of Hedgehog signaling pathway is mediated by the transmembrane proteins Patched (PTCH) and Smoothed (SMO) in multiple types of cancers [7]. The binding of Hedgehog signal to PTCH relieves SMO inhibition, which subsequently activates the transcription factors of glioma-associated oncogene (Gli) family (Gli1,

Posaconazole inhibited embryonal rhabdomyosarcoma

Gli2 and Gli3). As the nuclear executor, the Gli transcription factors are responsible for regulating the expressions of the downstream target genes [8, 9]. Inhibition of Hedgehog pathway could reduce cell proliferation and induce autophagy in non-Hodgkin lymphoma, chronic myeloid leukemia, and colon cancer [10-12]. The development and progression of ERMS are closely related to the consistent activation of Hedgehog signaling pathway and increasing evidence indicates that novel strategies targeting the Hedgehog pathway will be promising therapeutics for patients with ERMS [7, 13].

Posaconazole (POS), a second-generation triazole antifungal drug, is a potent inhibitor of the Hedgehog signaling pathway, which has been redefined as an anti-tumor compound recently. Most studies have focused on the effect of POS on fungi, ignoring the role of POS in other diseases such as tumors. POS inhibits the Hedgehog signaling pathway by targeting the class Frizzled (Class F) G protein-coupled receptor SMO, which is a key transmembrane protein of the Hedgehog signaling. Notably, POS has been shown to be effective in several types of tumors through the Hedgehog signaling pathway [14], such as glioblastoma [15], acute myeloid leukemia [16], and basal cell carcinoma [17]. However, the effect of POS on ERMS remains to be determined.

This study was designed to investigate the potential effect of POS on Hedgehog signaling pathway in ERMS. There is currently no commercial cell line derived from bladder ERMS, so we tested the effect of POS on Hedgehog signaling using ERMS cell lines including RD, RMS-YM, and KYM-1. Firstly, we identified the abnormal expression of SMO in human bladder ERMS samples and ERMS cell lines. Then POS was demonstrated to decrease cell viability, trigger cell cycle arrest, and induce cell autophagy in ERMS cell lines. Furthermore, the in vivo experiment confirmed that POS inhibited tumor growth in a xenograft murine model of ERMS. These findings may provide a theoretical basis for POS as a novel anti-tumor agent against ERMS, or even bladder ERMS.

Materials and methods

Cell lines and cell culture

The cell lines (RD and KYM-1) derived from ERMS, were purchased from Japanese Colle-

ction of Research Bioresources Cell Bank (Ibaraki, Japan). The cell line (RMS-YM) derived from ERMS was obtained from Riken Cell Bank (Tsukuba, Japan). These three cell lines were cultured in RPMI-1640 medium (Gibco, Invitrogen, USA) supplemented with 10% fetal bovine serum (FBS, Gibco, USA) and 1% penicillin/streptomycin (Gibco, USA). The cells were maintained in a humidified incubator at 37°C with 5% CO₂.

Reagents and antibodies

POS was purchased from MedChemExpress (MCE, New Jersey, USA), and its molecular structure is shown in **Figure 1D**. POS was dissolved in dimethyl sulfoxide (DMSO) to a formation of 10 mM stock solution for the in vitro experiments. The primary antibodies for Western Blot analysis were as follows: β -actin (CST, #4970, 1:1000), Gli1 (Santa Cruz Biotechnology, sc-515751, 1:800), SMO (Proteintech, 20787-1-AP, 1:1000), p21^{Waf1/Cip1} (CST, #2947, 1:1000), c-Myc (CST, #18583, 1:1000), CDK4 (CST, #2906, 1:1000), CDK6 (CST, #3136, 1:1000), Atg5 (CST, #9980, 1:1000), Beclin-1 (CST, #3495, 1:1000), LC3B (CST, #3868, 1:1000). The secondary antibodies were anti-rabbit IgG, HRP-linked Antibody (1:2000, CST, #7074), and anti-mouse IgG, HRP-linked Antibody (CST, #7076, 1:2000). SMO antibody (Proteintech, 20787-1-AP, 1:200) was used for the immunohistochemistry, LC3B antibody (CST, #3868, 1:500) was used for immunofluorescence staining.

XTT cell viability assay

Cell viability was detected by the XTT assay (Roche Diagnostics, USA). ERMS cells (1,000-3,000/well) were seeded in a 96-well plate and allowed to attach overnight. Then the cells were incubated with POS at concentrations ranging from 0 to 100 μ M for 24, 48 and 72 h. At the indicated time point, XTT reagent was added and then incubated for 4 to 24 h. The optical density (OD) levels were determined using a microplate reader (model 680; Bio-Rad Laboratories, Inc., USA).

Western blot analysis

ERMS cells were seeded in 6-well plates and treated with POS (0, 10 and 25 μ M) for 24 h according to the results of XTT assay. Then the treated cells were lysed in ice-cold lysis buffer

Posaconazole inhibited embryonal rhabdomyosarcoma

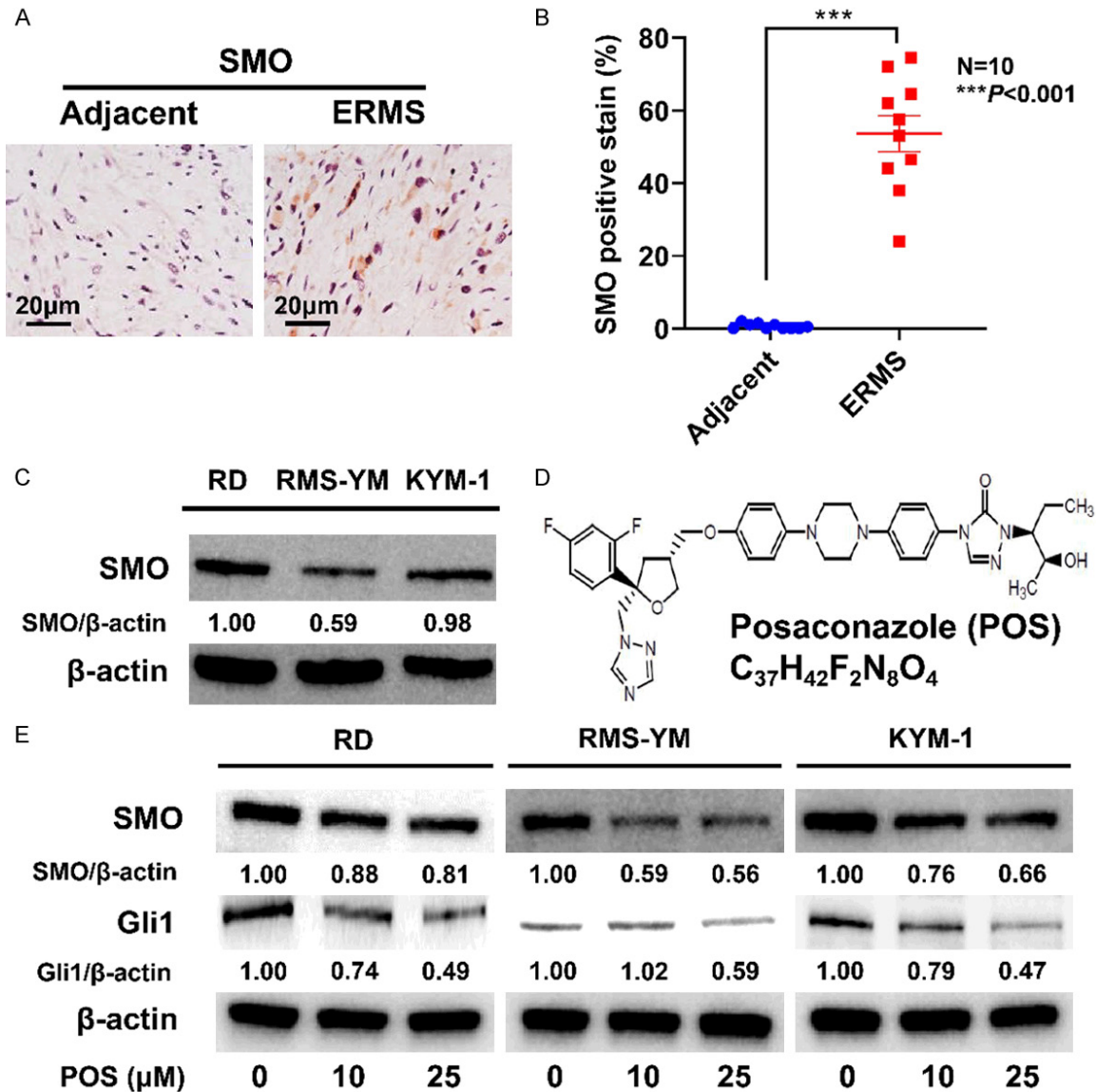


Figure 1. SMO expressed in bladder ERMS and POS inhibits Hedgehog signaling pathway in ERMS cells. A. Representative images of immunohistochemical staining for SMO in the tumor sections from human bladder ERMS tissues. Scale bar =20 μm. B. The SMO positive rate of bladder ERMS tissues (ten cases) was significantly higher than that of adjacent non-tumor tissues (ten cases). Data are presented as mean ± SD. N=10, ***P<0.001 vs. the adjacent group. C. SMO expressions in RD, RMS-YM, and KYM-1 cell lines. D. The chemical structure of POS. E. POS treatment for 24 h reduced the levels of SMO and Gli1 in ERMS cell lines. β-actin expression was regarded as an internal reference.

which contained protease and phosphatase inhibitor cocktail (#78501, Thermo Scientific, USA). Protein samples were separated by 10% or 12% SDS/polyacrylamide gel (Bio-Rad, Hercules, CA, USA) electrophoresis and then transferred to polyvinylidene difluoride membrane. The membrane was incubated with primary antibodies at 4°C overnight. The next day, the membrane was washed for 3-5 times

and then incubated with the corresponding secondary antibody at room temperature for 1 h. Finally, the immunoblots were visualized by the enhanced chemiluminescence (ECL) kit (Amersham Pharmacia Biotech, USA) and ChemiDoc Imaging System (Bio-Rad, USA). β-actin were regarded as the internal reference. The expression level of proteins was quantified by ImageJ software.

Posaconazole inhibited embryonal rhabdomyosarcoma

Cell cycle distribution analysis

According to the instructions for the Cell Cycle Analysis kit (BD Biosciences, San Jose, CA, USA), ERMS cells (3×10^5 /well) were seeded in a 6-well plate overnight, and then incubated with the fresh media with 10 μ M POS. Following 24 h treatment, the cells were harvested and then fixed with pre-cooled 70% ethanol. The next day, the fixed cells were washed twice in order to remove the residual ethanol (the first wash with PBS and the second one with the stain buffer (#554656, BD Biosciences). Subsequently, the cells were resuspended with PI/RNase staining buffer (#550-825, BD Biosciences). The cells could be further incubated for 15 min and then analyzed by the MACSQuant Analyzer 10 (Miltenyi Biotec, Germany).

Transmission electron microscopy (TEM) observation

ERMS cells were seeded in 6-well plates at 3×10^5 per well overnight, followed by 24 h incubation with the fresh media containing 25 μ M POS. The harvested cells were fixed in 2% glutaraldehyde at 4°C overnight. Subsequently, they were rinsed with PBS twice and then fixed with 1% osmium tetroxide for 3 h. The cell samples were next dehydrated using an ascending acetone series, followed by embedding and gradient polymerization. Next, the ultrathin sections were prepared and double-stained with uranyl acetate and lead citrate. The autophagic structures in POS-treated ERMS cells were observed under H-7650 transmission electron microscope (Hitachi Co., Japan).

Immunofluorescence staining

ERMS cells were plated on a glass-bottom dish and cultured overnight. After incubation with 25 μ M POS for 24 h, the cells were fixed with 4% formaldehyde at room temperature for 15 min, and then rinsed with PBS. Subsequently, they were incubated with LC3B antibody in a humidified chamber at 4°C overnight. The next day, after washing with PBS three times for 5 min each, the cells were treated with the fluorescent-labeled secondary antibody for 1 h at room temperature in dark. Finally, the nuclei were counterstained with DAPI, followed by examination and photography through a fluorescence microscope. Image J software was

applied to quantify the number of LC3B puncta per cell from five random fields of view.

ERMS subcutaneous implantation in SCID mice

RD cells (1×10^7) were suspended in 50 μ L Hank's balanced salt solution and 50 μ L Matrigel (#356234, BD Biosciences, USA), and then subcutaneously inoculated into the left rear flank of SCID mice. Once the tumor volume reached about 100 mm³, the mice were randomized into two groups (six mice per group), and orally received vehicle or POS (70 mg/kg) every day for 2 weeks before sacrifice. The tumor volume was measured with a caliper and then recorded twice every week. In the final stage of animal experiment, blood samples were collected for the serum analysis of liver function indicators such as glutamic-oxaloacetic transaminase (GOT) and glutamic-pyruvic transaminase (GPT). The tumor tissues were surgically resected and used for subsequent immunohistochemistry, and hematoxylin-eosin (HE) staining. All procedures of this animal experiment were approved by the Okayama University Ethics Committee.

Human bladder ERMS specimens

The tissue samples were collected after surgery, and pathologically diagnosed as bladder ERMS at Zhujiang Hospital. The specimens (ten cases) were matched with adjacent non-tumor tissues (ten cases) for comparison. After the tissues were cut into 4 μ m sections, they were then fixed in formalin, and embedded in paraffin to assess the expression of SMO. The study protocol was approved by the Medical Ethics Committee of Zhujiang Hospital. Informed consents were signed, and obtained from all the subjects.

Immunohistochemistry staining

The tumor tissue was removed, fixed in the formalin, and then embedded in the paraffin. After deparaffinization by xylene, the sections were rehydrated in a graded series of ethanol. Subsequently, the antigen retrieval was conducted by autoclave treatment in 10 mM pH 6.0 sodium citrate buffer at 120°C for 20 min. The 3% Hydrogen Peroxide (H₂O₂) was used to block the endogenous peroxidase activity for 10 min. To prevent non-specific staining, the sections were placed in 10% normal goat

Posaconazole inhibited embryonal rhabdomyosarcoma

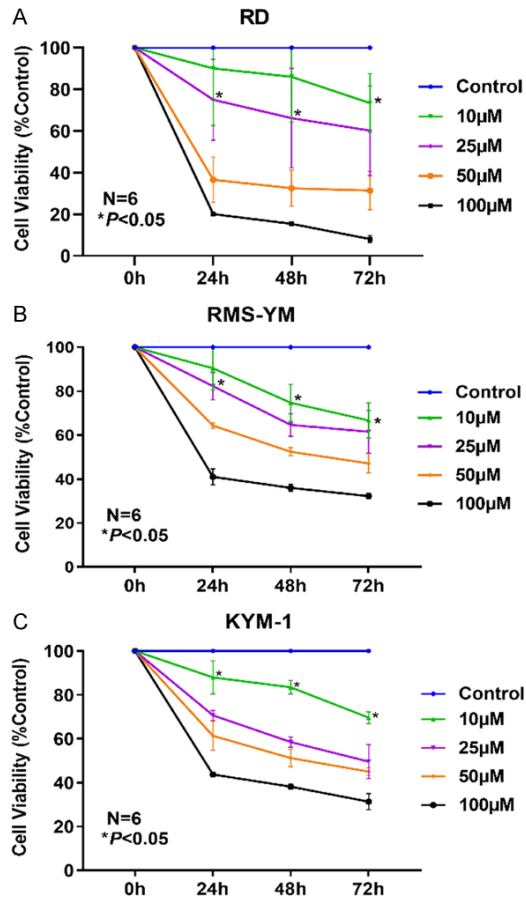


Figure 2. POS suppresses cell viability in human ERMS cells. XTT assay was performed to assess the effect of POS on the cell viability of RMS cell lines. POS inhibited the cell viability of (A) RD, (B) RMS-YM, and (C) KYM-1 in a time- and concentration-dependent manner. Data are presented as mean \pm SD. N=6, *P<0.05 vs. the control group.

serum solution for 40 min. Tissue sections were then incubated with SMO antibody (Proteintech, #20787-1-AP, 1:200), at 4°C overnight. After washed by PBS, the sections were then incubated with the secondary antibody at room temperature for 30 min. The DAB substrate kits (425312F, Nichirei Bioscience Inc.) were used for staining and the sections were then lightly counterstained by hematoxylin. Finally, the sections were observed and photographed under a microscope. The SMO positive rate was calculated from ten random fields of view.

Statistical analysis

All experiments were repeated independently for at least three times and all the data were presented as mean \pm standard deviation (SD).

The statistical data were processed by Graph-Pad Prism 8 software. Between-group variances were assessed with one-way or two-way analysis of variance, and the P value <0.05 was regarded as statistical significance.

Results

Overexpression of SMO in bladder ERMS specimens

The previous study has demonstrated the expression of SMO in RMS specimens [18]. To date, there have been no studies reporting SMO expression in bladder ERMS. In this study, SMO expression in bladder ERMS was evaluated by immunohistochemistry staining. As shown in **Figure 1A**, SMO was significantly overexpressed in bladder ERMS samples compared to paired adjacent non-tumor tissues. The SMO positive rate of bladder ERMS tissues was significantly higher than that of adjacent non-tumor tissues (**Figure 1B**).

POS inhibits Hedgehog signaling pathway

SMO expression was firstly identified in RD, RMS-YM, and KYM-1 cell lines (**Figure 1C**). SMO and Gli1 were then selected as the representatives to confirm the inhibitory effect of POS on Hedgehog signaling pathway. As shown in **Figure 1E**, POS downregulated the expressions of SMO and Gli1 in a concentration-dependent manner.

POS suppresses the cell viability of ERMS cell lines

XTT assay was conducted to assess the effect of POS on the cell viability of ERMS cell lines. RD, RMS-YM and KYM-1 cells were treated with different concentrations of POS (0, 10, 25, 50, and 100 µM) for 24, 48, and 72 h. As shown in **Figure 2A-C**, POS inhibited the cell viability of three ERMS cell lines in a time- and concentration-dependent manner. The half-maximal inhibitory concentration (IC50) of POS at 24 h was 36.51 µM and 62.62 µM for RD and RMS-YM cells, respectively. And RD cells were more sensitive to POS than RMS-YM and KYM-1 cells.

POS triggers G0/G1 cell cycle arrest in ERMS cell lines

After treated with 10 µM POS for 24 h, a higher percentage of RD, RMS-YM and KYM-1 cells

Posaconazole inhibited embryonal rhabdomyosarcoma

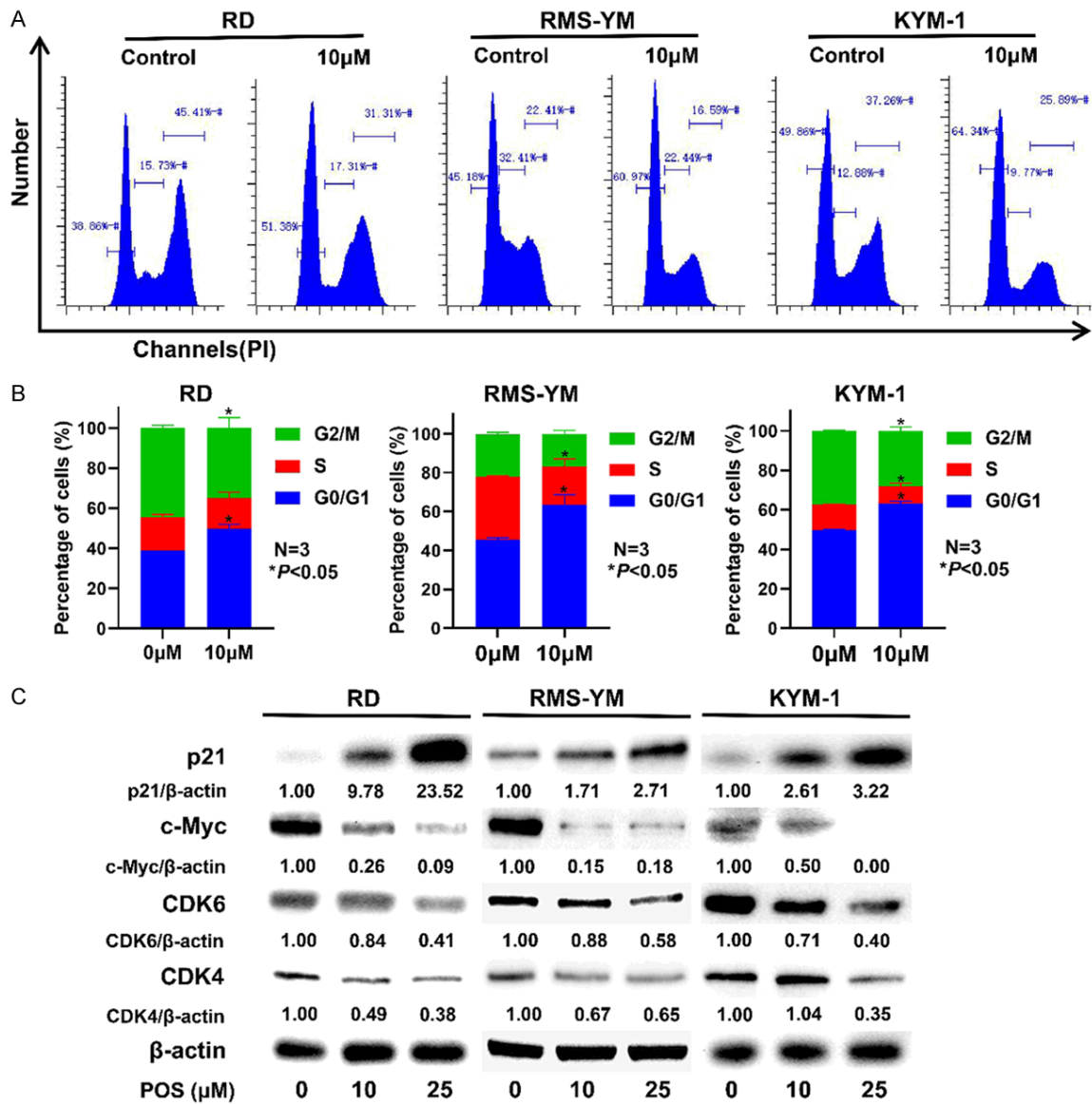


Figure 3. POS triggers G0/G1 cell cycle arrest in RD, RMS-YM, and KYM-1 cells. **A.** RD, RMS-YM, and KYM-1 cells were treated with 10 μM POS for 24 h, and then stained with PI/RNase. Flow cytometry was performed to analyze the cell cycle distribution. **B.** The percentages of RD, RMS-YM, KYM-E cells in G0/G1, S and G2/M phases are calculated based on the flow cytometric analysis. Data are presented as mean ± SD. N=3, *P<0.05 vs. the control group. **C.** RD, RMS-YM, and KYM-1 cells were treated with POS (0 μM, 10 μM and 25 μM) for 24 h. Western blot analysis indicated that POS upregulated the expression of p21^{Waf1/Cip1} while decreased the levels of c-Myc, CDK4, and CDK6. β-actin expression was regarded as an internal reference.

stayed at G0/G1 phase was found in the treatment group compared with the control group (Figure 3A, 3B). Subsequently, in order to elucidate the molecular mechanism of POS-induced cell cycle arrest, we further measured the cell cycle related proteins through western blot after ERMS cells were treated with POS (10 and 25 μM). POS was found to effectively upregulate the expression of p21^{Waf1/Cip1}, while POS downregulated c-Myc, CDK4, and CDK6

in a concentration-dependent manner (Figure 3C). The results above indicated that POS induces G0/G1 phase arrest in RD, RMS-YM, and KYM-1 cells.

POS induces cell autophagy in ERMS cell lines

Several studies have reported that the inhibition of Hedgehog signaling pathway is closely related to the occurrence of autophagy [19-

21]. Hence, we tried to determine whether POS could induce autophagy in ERMS cell lines under TEM. For all three ERMS cell lines, significant autophagosome formation was observed in the treatment group (**Figure 4A**). Afterwards, immunofluorescence staining for LC3B was performed in RD and RMS-YM cells, and the results indicated that the number of LC3B puncta per cell significantly increased with the treatment of 25 μ M POS (**Figure 4B, 4C**). To further prove our assumption, western blot analysis was conducted to detect the expressions of autophagy related proteins. POS elevated the expressions of Atg5, Beclin-1, and LC3-II in a dose-dependent manner (**Figure 4D**).

Anti-tumor potential of POS in vivo

The ERMS xenograft mouse model of RD cells was established to assess the therapeutic effect of POS. Tumor-bearing mice were orally administered with vehicle or POS (70 mg/kg) every day for 2 weeks. The representative change of tumor size (**Figure 5A**) in mice treated with POS was significantly lower than that in the control group. The average tumor weight was (0.598 \pm 0.241) g in the control group, and (0.150 \pm 0.051) g in treatment group (**Figure 5B**). Following two-week treatment, the tumor volume grew slowly in POS group when compared to the control group (**Figure 5C**). HE staining was conducted to examine the histopathological morphological changes. The tumor cells in POS group were characterized by disappeared nuclei and tumor necrosis, while those in vehicle group showed deeply stained, large and abnormal nuclei in intact cells (**Figure 5D**). Through HE staining performance in **Figure 5E**, POS could cause a certain extent of liver damage compared to vehicle group. For the analysis of liver function, no statistical difference was found in GOT (**Figure 5F**) and GPT (**Figure 5G**) after POS treatment, but the mean value of GPT in POS group was higher than that in vehicle group.

Discussion

As second-generation triazole antifungal drug, POS has exhibited certain anti-tumor properties and repurposed as an anti-tumor compound in recent years [17]. Our results demonstrated that POS suppressed cell viability, induced G0/G1 cell cycle arrest and autophagy

in ERMS cells through inhibition of Hedgehog signaling pathway. Through the downregulation of SMO and Gli1 detected by western blot, POS was found to effectively inhibit the Hedgehog signaling pathway. XTT assay indicated that POS inhibited the proliferation of human ERMS cell lines including RD (ERMS from pelvis), RMS-YM (ERMS from urachus), and KYM-1 (ERMS from neck), in a time- and concentration-dependent manner. For in vitro experiments, we selected the concentrations (10, 25 μ M) below IC50 according to cell viability assay, pre-experiment basis, and the related literatures [13, 17] of conventional Hedgehog inhibitors.

Arrest of tumor cell cycle progression has been regarded as promising in tumor treatment [22]. Regulation of embryonic development is the main role of Hedgehog signaling pathway and regulation of proliferation is the most basic function of Hedgehog signaling pathway [23]. Previous studies have shown that Hedgehog signaling pathway could alter the distribution of tumor cell cycle [12, 24]. In this study, flow cytometry demonstrated that the proportion of ERMS cells at G0/G1 stage increased significantly after POS treatment. More tumor cells were arrested at G0/G1 phase would result in impaired DNA replication, thus reducing the proliferation ability of ERMS cells. Western blot revealed that the expression of p21^{Waf1/Cip1} was significantly upregulated, while the expressions of c-Myc, CDK4, and CDK6 were downregulated following POS treatment. p21 is a classic p53-regulated cell cycle inhibitor and c-Myc plays a crucial role in sustaining the proliferation of human tumor cells, which promotes the cell cycle progression from G1 to S stage. Cyclin-dependent kinases 4/6 (CDK4/CDK6) are the downstream cell cycle regulators of p21, which can promote the transition from G0 to G1 phase [25]. Our data suggest that POS treatment could prevent the transition from G0 into G1 phase by downregulating the expressions of CDK4 and CDK6, which were regulated by p53/c-Myc/p21 signals.

Autophagy involves the delicately regulated catabolic digestion of damaged cell organelles and proteins mediated by lysosomes. Although the role of autophagy in tumors has not been definitely determined, accumulating evidence indicates that the induction of autophagy and inhibition of autophagosome degradation can

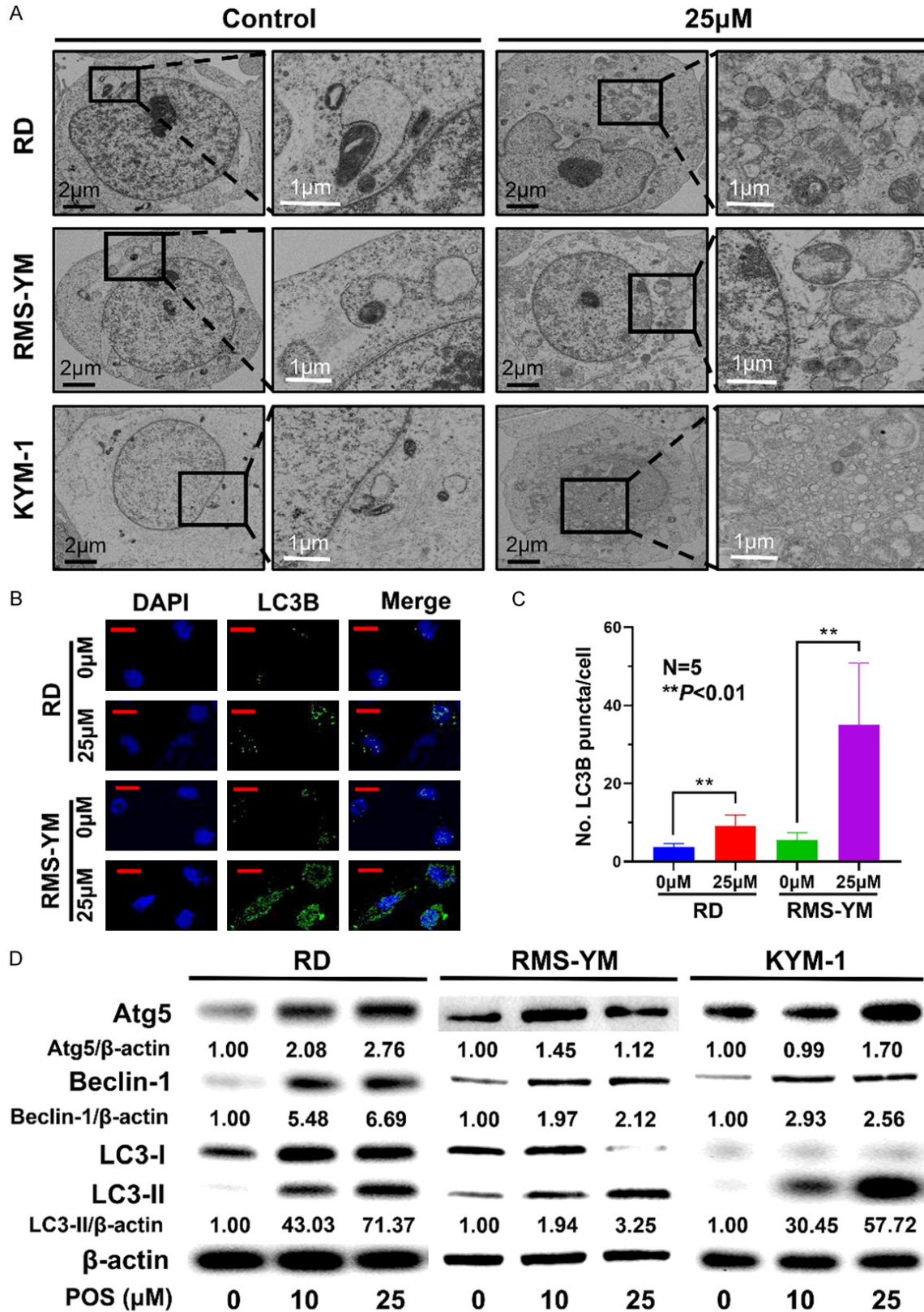


Figure 4. POS induces cellular autophagy in ERMS cells. **A.** RD, RMS-YM, and KYM-1 cells were treated with 25 μ M POS for 24 h. Representative images of autophagosome formation were observed by TEM analysis (black scale bar =2 μ m, white scale bar =1 μ m). **B.** The expressions of LC3B in RD and RMS-YM cells following 25 μ M POS treatment were detected by immunofluorescence staining (green) whereas the nuclei were stained with DAPI (blue). (Red

Posaconazole inhibited embryonal rhabdomyosarcoma

scale bar =20 μm). C. The number of LC3B puncta per cell from five random fields of view was quantified in RD and RMS-YM cells after 25 μM POS treatment. (N=5, ** $P < 0.01$). D. Western blot analysis of Atg5, Beclin-1, LC3-I, and LC3-II in RD, RMS-YM, and KYM-1 cells after POS treatment for 24 h. β -actin expression was regarded as an internal reference.

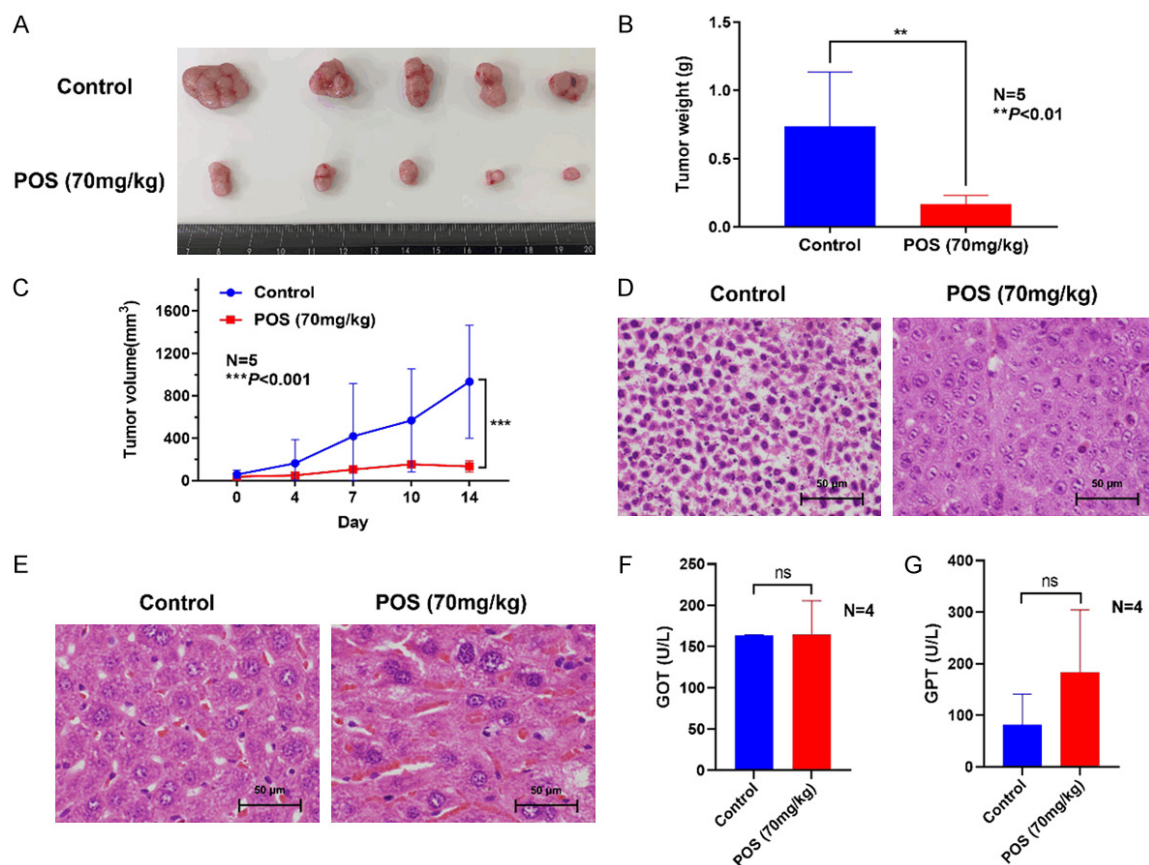


Figure 5. POS inhibits RD cell growth in vivo. A. Images of the resected ERMS tumors from mice were photographed after two-week treatment. B. The average weight of tumors in POS (70 mg/kg) group was significantly lower than that in the control group. Data are presented as mean \pm SD. N=5, ** $P < 0.01$ vs. the control group. C. The tumor volume was measured twice every week. Data are presented as mean \pm SD. N=5, *** $P < 0.001$ vs. the control group. D. HE staining of ERMS tissues indicated that the disappeared nuclei and tumor necrosis were identified in POS group, while the deeply stained, large and abnormal nuclei in intact cells were found in the control group. Scale bar =50 μm . E. HE staining of mice liver showed some liver impairment after POS treatment compared to the control group. Scale bar =50 μm . F, G. The analysis of liver function revealed no statistical difference in GOT and GPT between POS treatment group and control group, but mean GPT of the POS group was higher than that of control group. Data are presented as mean \pm SD. N=4, ns: not significant vs. the control group.

inhibit tumor progression. Several novel drugs have been identified to induce autophagic cell death (ACD), which are regarded as promising anti-tumor therapy [26]. The process of autophagy is mediated by a series of autophagy-related genes (ATG). The formation of double-membrane vesicles, termed as autophagosomes, marks the beginning of autophagy. The microtubule-associated protein light chain 3 (LC3), especially the lipidated LC3-II, plays a key role in the initiation of autophagy process.

Beclin-1 (Atg6), a tumor suppressor gene, is generally downregulated in many different cancers, and promotes the formation or transportation of autophagosomes. The TEM images exhibited significant autophagosome formation of double-membrane autophagosomes in all three cell lines after POS treatment. The number of autophagic vacuoles (autophagosomes plus autolysosomes) in POS treatment group was visibly larger than that in control group. Western blot analysis revealed that POS

treatment upregulated the expressions of Atg5, Beclin-1, and LC3-II. The upregulation of these proteins verified the occurrence of autophagy in ERMS cells following POS treatment. Subsequently, immunofluorescence staining was performed to confirm the number of LC3B puncta per cell in RD and RMS-YM cells, which distinctly increased after POS treatment.

Hedgehog signaling pathway has significant implications in the regulation of cell cycle and autophagy. Gli proteins may serve as both transcriptional activators and repressors in the Hedgehog signaling pathway. In the absence of Hedgehog Signaling, the C-terminally truncated Gli2/3 function as the transcriptional repressors while Gli1 is generally considered to be a transcriptional activator [27]. Gli1 is regarded as a protooncogenic role in a series of cancers and plays a certain role in the cancer stem cell maintenance. When the Hedgehog signaling pathway is activated, Gli proteins cannot be phosphorylated and degraded so that they remain the Gli-activated form (GliA). While the active Gli2/3 would promote the expression and transcription of Gli1, thus promoting tumorigenesis [28]. Gli1 has been applied as a biomarker to determine the activation of Hedgehog signaling pathway [27, 28]. In addition, previous studies have revealed that Gli1 can regulate the cell cycle progression [29] and the process of cell autophagy [30]. Therefore, we chose to analyze the expression level of Gli1 to assess the inhibitory effect of POS on Hedgehog signaling pathway. The previous study has indicated that Hedgehog signaling negatively regulates the expression of p53-independent p21^{Waf1/Cip1} through Gli1, thereby affecting the cell cycle transition from G1 to S phase [24]. Cellular autophagy can be impaired by the overexpressions of PTCH or SMO. The transmembrane protein SMO receptor plays an essential role in Hedgehog pathway-regulated autophagy as SMO protein modulates the synthesis of autophagosomes [31]. For the above reasons, we detected the key proteins of Hedgehog signaling pathway, including SMO and Gli1, which not only proved the inhibitory effect of POS on Hedgehog signaling pathway, but also further confirmed the upstream pathway components in the regulation of cell cycle arrest and cellular autophagy (Figure 6). The tumors grew more slowly in the treatment group than in the control group, re-

vealing that POS (70 mg/kg) had an effective anti-tumor potency in ERMS xenograft mice model. Consistently, the tumor cells in POS group were characterized by disappeared nuclei and tumor necrosis.

Traditional inhibitors of Hedgehog signaling pathway may have some problems and limitations when applied as anti-tumor drugs or anti-RMS drugs. As is shown in relevant study [32], the classical Hedgehog signaling pathway inhibitors, such as Cyclopamine, Vismodegib, and Sonidegib, with high concentrations, may lead to off-target effect on Gli1 expression in certain RMS cell lines, which impedes the research path of targeting Hedgehog signaling pathway for the treatment of RMS to some extent. Actually, the occurrence of off-target effect is highly correlated with the mechanism of action and pharmacokinetics, certain cell lines and drug concentrations so that the anti-tumor effects of different inhibitors targeting Hedgehog signaling pathway are diversified [13]. In this study, we couldn't completely prove whether POS treatment would cause the off-target effect on Gli1 expression, while no relevant studies have reported that POS has similar problems to traditional inhibitors. Moreover, POS has been verified to inhibit Hedgehog signaling pathway at distinct sites from other traditional Hedgehog signaling pathway inhibitors, revealing that the action mechanism of POS is different from traditional inhibitors [17]. Our results demonstrated that Gli1 expressions in three ERMS cell lines from different tissue origins were dose-dependently downregulated with POS treatment of 10 μ M and 25 μ M, showing the consistent experimental results in different cell lines under the same concentrations of POS. Therefore, we believe that POS would not lead to off-target effect on Gli1 expression at least in the used concentration range. Meanwhile, traditional SMO inhibitors have relatively severe side effects, while the novel SMO inhibitor POS possesses the advantages of few drug interactions and less damage to liver and kidney function, and even the potentials against drug-resistant SMO mutants, which ensures its potential use as a long-term medication for tumor treatment [33]. In ERMS xenograft SCID mice model, POS therapy could cause some liver impairment by HE staining, and increase mean GPT, but there was no statistical differ-

Posaconazole inhibited embryonal rhabdomyosarcoma

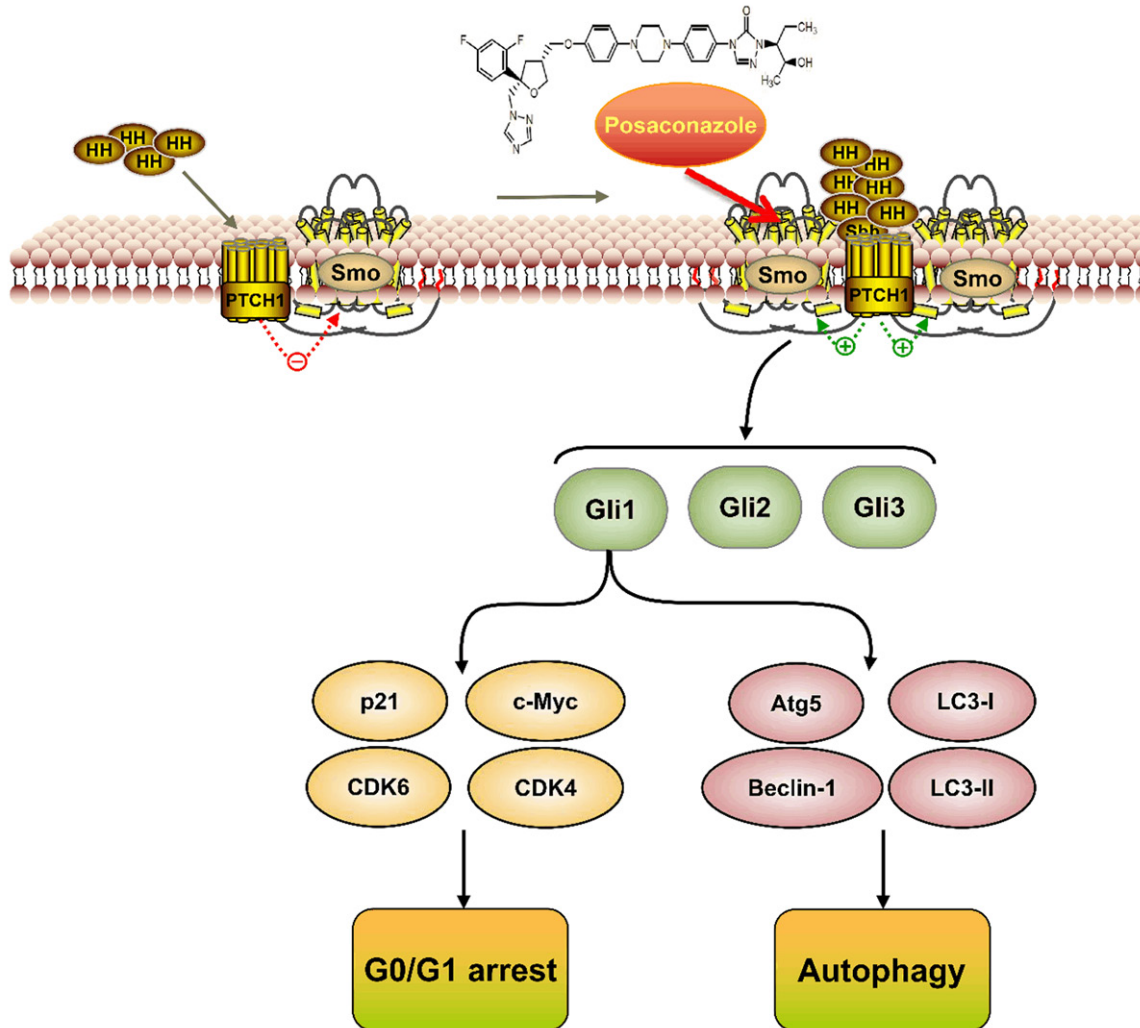


Figure 6. The schema elucidates the mechanism underlying POS-induced G0/G1 arrest and autophagy in ERMS cells.

ence in GOT. Thus, more preclinical studies are required to verify the effect of POS at different doses on liver function. The high expression of SMO in bladder ERMS indicates that therapy targeting SMO in Hedgehog signaling pathway may be a promising strategy. The dynamic subcellular distributions of SMO in ERMS cells over a time course [34], more preclinical and clinical studies are needed to better elucidate the role of POS as a potential agent against bladder ERMS.

In summary, our findings imply that POS suppresses cell viability and induces G0/G1 cell cycle arrest and autophagy in three ERMS cell lines through inhibition of Hedgehog signaling pathway. Moreover, our proposal might also be applicable in bladder ERMS treatment with

POS. Hence, POS may be a potent therapeutic agent to inhibit ERMS, even bladder ERMS through targeting SMO in Hedgehog signaling pathway.

Acknowledgements

This research was funded by the Mobility Programme of National Natural Science Foundation of China (M-0299) and the Ministry of Education, Culture, Sports, Science and Technology of Japan (grant No. 17K11138, 21K09371). We thank Hideo Ueki and Shunai Li at Okayama University for their technical guidance.

Disclosure of conflict of interest

None.

Abbreviations

POS, posaconazole; RMS, rhabdomyosarcoma; ERMS, embryonal rhabdomyosarcoma; ARMS, Alveolar rhabdomyosarcoma; PTCH, patched; SMO, smoothened; Gli, glioma-associated oncogene; FBS, fetal bovine serum; DMSO, dimethyl sulfoxide; CDK4/6, cyclin-dependent kinase 4/6; Atg, autophagy-related proteins; LC3, light chain 3; TEM, transmission electron microscopy; SCID, severe combined immune deficiency; GOT, glutamic-oxaloacetic transaminase; GPT, glutamic-pyruvic transaminase; HE staining, hematoxylin-eosin staining; SD, standard deviation; IC50, half-maximal inhibitory concentration; ACD, autophagic cell death.

Address correspondence to: Dr. Peng Huang, Department of Urology, Okayama University Graduate School of Medicine, Dentistry and Pharmaceutical Sciences, Okayama, Japan. Tel: +81-86-235-7997; Fax: +81-86-235-7884; E-mail: huangpeng509@gmail.com; Dr. Abai Xu, Department of Urology, Zhujiang Hospital, Southern Medical University, Guangzhou, China. Tel: +86-20-62782739; E-mail: lc96xab@163.com

References

[1] Miwa S, Yamamoto N, Hayashi K, Takeuchi A, Igarashi K and Tsuchiya H. Recent advances and challenges in the treatment of rhabdomyosarcoma. *Cancers (Basel)* 2020; 12: 1758.

[2] van Erp AEM, Versleijen-Jonkers YMH, van der Graaf WTA and Fleuren EDG. Targeted therapy-based combination treatment in rhabdomyosarcoma. *Mol Cancer Ther* 2018; 17: 1365-1380.

[3] Castagnetti M, Herbst KW and Esposito C. Current treatment of pediatric bladder and prostate rhabdomyosarcoma (bladder preserving vs. radical cystectomy). *Curr Opin Urol* 2019; 29: 487-492.

[4] Shrestha R, Mohankumar K and Safe S. Bisindole derived nuclear receptor 4A1 (NR4A1) antagonists inhibit TGFbeta-induced invasion of embryonal rhabdomyosarcoma cells. *Am J Cancer Res* 2020; 10: 2495-2509.

[5] Mo J, Liu F, Sun X, Huang H, Tan K, Zhao X, Li R, Jiang W, Sui Y, Chen X, Shen K, Zhang L, Ma J, Zhao K and Tang Y. Inhibition of the FACT complex targets aberrant hedgehog signaling and overcomes resistance to smoothened antagonists. *Cancer Res* 2021; 81: 3105-3120.

[6] Steele NG, Biffi G, Kemp SB, Zhang Y, Drouillard D, Syu L, Hao Y, Oni TE, Brosnan E, Elyada

E, Doshi A, Hansma C, Espinoza C, Abbas A, The S, Irizarry-Negron V, Halbrook CJ, Franks NE, Hoffman MT, Brown K, Carpenter ES, Nwosu ZC, Johnson C, Lima F, Anderson MA, Park Y, Crawford HC, Lyssiotis CA, Frankel TL, Rao A, Bednar F, Dlugosz AA, Preall JB, Tuveson DA, Allen BL and Pasca di Magliano M. Inhibition of hedgehog signaling alters fibroblast composition in pancreatic cancer. *Clin Cancer Res* 2021; 27: 2023-2037.

[7] Cortes JE, Gutzmer R, Kieran MW and Solomon JA. Hedgehog signaling inhibitors in solid and hematological cancers. *Cancer Treat Rev* 2019; 76: 41-50.

[8] Pietrobono S, Gagliardi S and Stecca B. Non-canonical hedgehog signaling pathway in cancer: activation of gli transcription factors beyond smoothened. *Front Genet* 2019; 10: 556.

[9] Grunewald TG, Alonso M, Avnet S, Banito A, Burdach S, Cidre-Aranaz F, Di Pompo G, Distel M, Dorado-Garcia H, Garcia-Castro J, Gonzalez-Gonzalez L, Grigoriadis AE, Kasan M, Koelsche C, Krumbholz M, Lecanda F, Lemma S, Longo DL, Madrigal-Esquivel C, Morales-Molina A, Musa J, Ohmura S, Ory B, Pereira-Silva M, Perut F, Rodriguez R, Seeling C, Al Shaaili N, Shaabani S, Shiavone K, Sinha S, Tomazou EM, Trautmann M, Vela M, Versleijen-Jonkers YM, Visgauss J, Zalacain M, Schober SJ, Lissat A, English WR, Baldini N and Heymann D. Sarcoma treatment in the era of molecular medicine. *EMBO Mol Med* 2020; 12: e111131.

[10] Yang L, Shi P, Zhao G, Xu J, Peng W, Zhang J, Zhang G, Wang X, Dong Z, Chen F and Cui H. Targeting cancer stem cell pathways for cancer therapy. *Signal Transduct Target Ther* 2020; 5: 8.

[11] Chang H and Zou Z. Targeting autophagy to overcome drug resistance: further developments. *J Hematol Oncol* 2020; 13: 159.

[12] Deng H, Huang L, Liao Z, Liu M, Li Q and Xu R. Itraconazole inhibits the Hedgehog signaling pathway thereby inducing autophagy-mediated apoptosis of colon cancer cells. *Cell Death Dis* 2020; 11: 539.

[13] Ridzewski R, Rettberg D, Dittmann K, Cuvelier N, Fulda S and Hahn H. Hedgehog inhibitors in rhabdomyosarcoma: a comparison of four compounds and responsiveness of four cell lines. *Front Oncol* 2015; 5: 130.

[14] Teske KA, Dash RC, Morel SR, Chau LQ, Wechsler-Reya RJ and Hadden MK. Development of posaconazole-based analogues as hedgehog signaling pathway inhibitors. *Eur J Med Chem* 2019; 163: 320-332.

[15] Agnihotri S, Mansouri S, Burrell K, Li M, Matmatjan Y, Liu J, Nejad R, Kumar S, Jalali S, Singh SK, Vartanian A, Chen EX, Karimi S, Singh O, Bunda S, Mansouri A, Aldape KD and

Posaconazole inhibited embryonal rhabdomyosarcoma

- Zadeh G. Ketoconazole and posaconazole selectively target HK2-expressing glioblastoma cells. *Clin Cancer Res* 2019; 25: 844-855.
- [16] Agarwal SK, DiNardo CD, Potluri J, Dunbar M, Kantarjian HM, Humerickhouse RA, Wong SL, Menon RM, Konopleva MY and Salem AH. Management of venetoclax-posaconazole interaction in acute myeloid leukemia patients: evaluation of dose adjustments. *Clin Ther* 2017; 39: 359-367.
- [17] Chen B, Trang V, Lee A, Williams NS, Wilson AN, Epstein EH Jr, Tang JY and Kim J. Posaconazole, a second-generation triazole antifungal drug, inhibits the hedgehog signaling pathway and progression of basal cell carcinoma. *Mol Cancer Ther* 2016; 15: 866-876.
- [18] Arnhold V, Boos J and Lanvers-Kaminsky C. Targeting hedgehog signaling pathway in pediatric tumors: in vitro evaluation of SMO and GLI inhibitors. *Cancer Chemother Pharmacol* 2016; 77: 495-505.
- [19] Wang Y, Han C, Lu L, Magliato S and Wu T. Hedgehog signaling pathway regulates autophagy in human hepatocellular carcinoma cells. *Hepatology* 2013; 58: 995-1010.
- [20] Zeng X and Ju D. Hedgehog signaling pathway and autophagy in cancer. *Int J Mol Sci* 2018; 19: 2279.
- [21] Fan J, Zhang X, Wang S, Chen W, Li Y, Zeng X, Wang Y, Luan J, Li L, Wang Z, Sun X, Shen B and Ju D. Regulating autophagy facilitated therapeutic efficacy of the sonic hedgehog pathway inhibition on lung adenocarcinoma through GLI2 suppression and ROS production. *Cell Death Dis* 2019; 10: 626.
- [22] Hwang JW, Cho Y, Bae GU, Kim SN and Kim YK. Protein arginine methyltransferases: promising targets for cancer therapy. *Exp Mol Med* 2021; 53: 788-808.
- [23] Ho EK, Tsai AE and Stearns T. Transient primary cilia mediate robust hedgehog pathway-dependent cell cycle control. *Curr Biol* 2020; 30: 2829-2835, e2825.
- [24] Kumar V, Vashishta M, Kong L, Wu X, Lu JJ, Guha C and Dwarakanath BS. The role of notch, hedgehog, and Wnt signaling pathways in the resistance of tumors to anticancer therapies. *Front Cell Dev Biol* 2021; 9: 650772.
- [25] Hume S, Dianov GL and Ramadan K. A unified model for the G1/S cell cycle transition. *Nucleic Acids Res* 2020; 48: 12483-12501.
- [26] Jung S, Jeong H and Yu SW. Autophagy as a decisive process for cell death. *Exp Mol Med* 2020; 52: 921-930.
- [27] Aberger F and Ruiz i Altaba A. Context-dependent signal integration by the GLI code: the oncogenic load, pathways, modifiers and implications for cancer therapy. *Semin Cell Dev Biol* 2014; 33: 93-104.
- [28] Almazán-Moga A, Zarzosa P, Vidal I, Molist C, Giralt I, Navarro N, Soriano A, Segura MF, Alfranca A, Garcia-Castro J, Sánchez de Toledo J, Roma J and Gallego S. Hedgehog pathway inhibition hampers sphere and holoclone formation in rhabdomyosarcoma. *Stem Cells Int* 2017; 2017: 7507380.
- [29] Ohta M, Tateishi K, Kanai F, Watabe H, Kondo S, Guleng B, Tanaka Y, Asaoka Y, Jazag A, Imamura J, Ijichi H, Ikenoue T, Sata M, Miyagishi M, Taira K, Tada M, Kawabe T and Omata M. p53-independent negative regulation of p21/cyclin-dependent kinase-interacting protein 1 by the sonic hedgehog-glioma-associated oncogene 1 pathway in gastric carcinoma cells. *Cancer Res* 2005; 65: 10822-10829.
- [30] Sun Y, Guo W, Ren T, Liang W, Zhou W, Lu Q, Jiao G and Yan T. Gli1 inhibition suppressed cell growth and cell cycle progression and induced apoptosis as well as autophagy depending on ERK1/2 activity in human chondrosarcoma cells. *Cell Death Dis* 2014; 5: e979.
- [31] Cochrane CR, Vaghjiani V, Szczepny A, Jayasekara WSN, Gonzalez-Rajal A, Kikuchi K, McCaughan GW, Burgess A, Gough DJ, Watkins DN and Cain JE. Trp53 and Rb1 regulate autophagy and ligand-dependent hedgehog signaling. *J Clin Invest* 2020; 130: 4006-4018.
- [32] Curran T. Reproducibility of academic preclinical translational research: lessons from the development of hedgehog pathway inhibitors to treat cancer. *Open Biol* 2018; 8: 180098.
- [33] Yang T, Yang Y and Wang Y. Predictive biomarkers and potential drug combinations of epi-drugs in cancer therapy. *Clin Epigenetics* 2021; 13: 113.
- [34] Kotulak-Chrzaszcz A, Kmiec Z and Wierzbicki PM. Sonic hedgehog signaling pathway in gynecological and genitourinary cancer (review). *Int J Mol Med* 2021; 47: 106.